CALCULATION OF VELOCITY FIELD IN 3-D RANDOM WAVES

Yu-xiu Yu* and Ning-chuan Zhang**

ABSTRACT

A method simply treating the governing equation for 3-D wave-motion is proposed in this paper. The Euler's velocity in whole depth can be directly calculated with this method if the wave free surface is given. For the linear waves the wave surface is determined from given directional spectrum (Yu. et al. 1991) or other wave surfaces at near locations with an inversion method proposed in this paper. For the nonlinear waves the wave surface can be determined with the method proposed by Dommermuth and Yue (1987). These methods proposed by authors are tested and verified with numerical simulation, model test or field observation data.

1. INTRODUCTION

The sea wave is a three-dimentional random process. An understanding of the kinematics of waves is critical to the understanding of many processes in the sea from the forcing on structures to nearshore sediment transport. In general the velocity field of sea waves is three dimentional, random, and nonlinear. Due to the complexity of this problem, some scientists only considered its three-dimentionality and random property and the direct linear superposition method was used to calculated the velocity. Others emphasized its nonlinearity and the higher-order unidirectional wave theories were used. Forristall et al (1978) showed that even linear wave theory with directional spereading of wave energy predicts storm wave kinematics of the subsurface flow better than higher-order unidirectional wave theories. But the direct linear method greatly overestimate crest velocities near the surface (Donelan, 1992). Some methods, for example the coordinate stretching method and the extrapolation method were proposed to correct the direct linear method and the results of former are smaller than that of the latter. The measured kinematics in the crests of random waves is bounded by these two modified linear models

* Professor, The State Key Laboratory of Coastal and Offshore Engineering, Dalian University of Technology (DUT), Dalian 116024. China

** Associate Professor, Dept. of Civil Eng. DUT, Dalian 116024, China

(Roderbusch and Forristall, 1982). More recently, Donelan (1992) proposed a new method based on the linear superposition of a sum of freely propagating wavetrains and assume that shorter waves ride on longer ones. But the effect of nonlinearity is not considered yet in this method.

Methods used for the calculation of velocity field in irregular waves fall into two general categories, global and local approximations. The local method attempt to find separate salutions to the governing equations that fit sequential windows in time of the given record, rather than attempting to find a single solution that fits an entire record. The amount of computation work is large.

Prislin and Zhang (1997) presented a newly-developed deterministic methodology for decomposition of nonlinear short-crested irregular waves up to second order in wave steepness into a characteristic set of free-wave components. Based on the decomposed free-wave components, the Directional Hybrid Wave Method (DHWM) allows for prediction of wave properties other then measured and at different locations including wave crests.

Dommermuth and Yue (1987) developed a numerical method for modelling nonlinear gravity waves which is based on the Zakharov equation/mode-coupling idea but is generalized to include interactions up to an arbitrary order M in wave steepness. This method were used to calculate the deformation of a travelling wave (Dommermuth, et al. 1987). In this paper, an inversion method is proposed to determine the wave surface from other wave surfaces at near locations, then it is used as the boundary condition to derive the wave kinematics in 3-D random waves with Dommermuth's idea.

2. NUMERICAL INVERSION OF 3-D RANDOM WAVE SURFACE

The single direction per frequency model (Yu et. al. 1991) is used to describe the 3-D random wave surface at point (x, y):

$$\eta(x,y,t) = \sum_{m=1}^{M}\sum_{i=1}^{I} a_{mi}\cos[\omega_{mi}t + k_{mi}(x\cos\theta_i + y\sin\theta_i) + \varepsilon_{mi}] \tag{1}$$

$$a_{mi} = \sqrt{2S(\omega_m, \theta_i)d\omega_m d\theta_i} \tag{2}$$

where M and N are the division numbers of frequency and direction respectively; a_{mi}, ω_{mi}, k_{mi} and ε_{mi} are amplitude, frequency, wave number and random initial phase of the component waves; $S(\omega, \theta)$ is the directional spectrum.

Usually, if the directional spectrum is given, the 3-D wave surface can be obtained with Eqs. (1) and (2). It also can be measured. But sometimes we can not measure the wave surface at structure position. In this case, an inversion method is proposed to determined the wave surface from other wave surfaces at near locations. The wave surface can be expanded as a Fourier Series:

$$\eta(x,y,t) = \sum_{j=1}^{J}(A_j\cos\omega_j + B_j\sin\omega_j) \tag{3}$$

where A_j and B_j are the Fourier coefficients. If the length of the wave data is L, then

$$\left.\begin{aligned} A_j &= \frac{2}{L}\sum_{l=1}^{L}\eta(x,y,t_l)\cos\omega_j t_l dt \\ B_j &= \frac{2}{L}\sum_{l=1}^{L}\eta(x,y,t_l)\sin\omega_j t_l dt \end{aligned}\right\} \tag{4}$$

Eq. (3) can be rewrite as

$$\left.\begin{aligned} \eta(x,y,t) &= \sum_{j=1}^{J} a_j\cos(\omega_j t + \beta_j) \\ a_j &= \sqrt{A_j^2 + B_j^2} \\ \beta_j &= \arctan(-B_j/A_j) \end{aligned}\right\} \tag{5}$$

Comparing with Eq. (1) we can get the total phase

$$\beta_j = k_j(x\cos\theta_j + y\sin\theta_j) + \varepsilon_j$$

If the wave surfaces, $\eta(x,y,t)$ are measured at I points and $I \geqslant 3$, the total phase for each surfacr can be obtained

$$\left.\begin{aligned} \beta_j^1 &= k_j(x_1\cos\theta_j + y_1\sin\theta_j) + \varepsilon_j \\ \beta_j^2 &= k_j(x_2\cos\theta_j + y_2\sin\theta_j) + \varepsilon_j \\ &\vdots \\ \beta_j^I &= k_j(x_I\cos\theta_j + y_I\sin\theta_j) + \varepsilon_j,\ I \geqslant 3 \end{aligned}\right\} \tag{7}$$

In these equations, only the directions, θ_j and the initial phase ε_j of component waves are unknow and they can be obtained from any two equations in principle. For example, from points 1 and 2 (Fig. 1) one can get

$$\theta_{jk} = \alpha_{12} + \cos^{-1}\left(\frac{\beta_j^1 - \beta_j^2}{k_j D_{12}}\right) \tag{8}$$

But in Eqs. (5) and (8), both arctangent and arccosine are multi-value function. Moreover, some component wave's directions are nearly parallel to the line 1-2 and the Eq. (7) for points 1 and 2 is invalid for these component waves. Therefore, at least three measured points are necessary. For each pair of measured point, two equations form a simultaneous equations and the values of θ_j and ε_j can be obtained for each component wave except the invalid condition. In general, for n pairs of measured points.

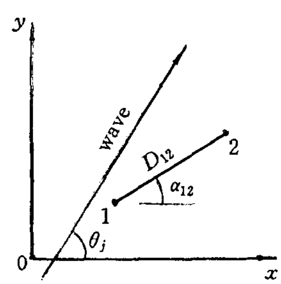

Fig. 1

$$\theta_j = \frac{1}{n}\sum_{k=1}^{n}\theta_{jk} \qquad n \geqslant 3 \tag{9}$$

Then the wave surface at any point can be calculated with Eq. (1) if the wave field is homogenous.

The numerical simulation, the physical simulation and the field wave data are used to examine this method. Five wave gages of vertical line type arranged in T-type array (Fig. 2a) were used in the field observation (Liu and Yu, 1995). The wave data were recorded simultaneously for 1200 seconds every hour and the time interval, Δt is 0.25s. Fig. 2(b) shows an example of the comparison of wave surfaces between field data at point 1 and the numerical inversion result form these at points 2, 3, 4 and 5. It shows that this method is successful and its precision is dependent on the length of data, $N\Delta t$, the distance, R from measured points to predicted point and the spatial homogeneity of wave field. According to the numerical simulation result, when $R/L_s = 1.0$, number of points $N \geqslant 2000$, when $R/L_s = 10$, $N \geqslant 3000$ and when $R/L_s = 20$, $N \geqslant 4000$, where L_s is the significant wave length. But in nature, the wave field is not exactly homogenous, so the validity of this method is limited to a few wave length from the measurement sites.

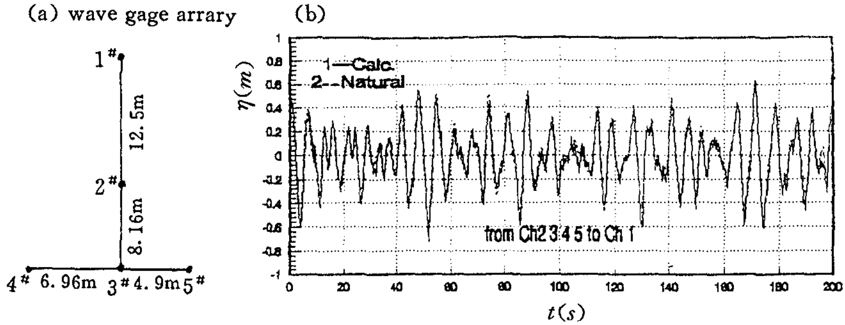

Fig. 2 A comparison of wave surfaces between field data (----) and numerical inversion (——)

3 CALCULATION OF VELOCITY FIELD

3.1 Governing Equations

The irrotational wave motion of a homogeneous, incompressible and inviscid fluid is considered. The origin is located at the mean water level and the vertical axis z is positive upward. The wave flow can be described by a velocity potential $\phi(x,y,z,t)$ such that within the fluid ϕ satisfies Laplace's equation:

$$\Delta\phi = \frac{\partial^2\phi}{\partial x^2} + \frac{\partial^2\phi}{\partial y^2} + \frac{\partial^2\phi}{\partial z^2} = 0 \tag{10}$$

$$x_s(y,t) \leqslant x \leqslant \infty;\ -\infty < y < \infty;\ -d(x,y) \leqslant z \leqslant \eta(x,y,t)$$

where $x_s(y,t)$ denote the coordinate x of boundary between water and land at time t. $\eta(x,y,t)$ is the free surface of wave. For determining the velocity potential, the following boundary conditions should be satisfied

Kinematics condition at bottom

$$\left.\frac{\partial\phi}{\partial\eta}\right|_{z=-d} = 0 \tag{11}$$

Kinematics condition at free surface

$$\left.\frac{\partial\phi}{\partial z}\right|_{z=\eta} = \frac{\partial\eta}{\partial t} + \frac{\partial\eta}{\partial x}\left.\frac{\partial\phi}{\partial x}\right|_{z=\eta} + \frac{\partial\eta}{\partial y}\left.\frac{\partial\phi}{\partial y}\right|_{z=\eta} \tag{12}$$

Dynamic condition at free surface

$$\left.\frac{\partial\phi}{\partial t}\right|_{z=\eta} + g\eta + \frac{1}{2}(\nabla\phi \cdot \nabla\phi|_{z=\eta}) + \frac{p_s(x,y,t)}{\rho} = 0 \tag{13}$$

$x \to \infty$ or $y \to \infty$ or $z \leftarrow \infty$; $\phi(x,y,z,t)$ and $\eta(x,y,t)$ are finite.

Initial condition

$$\eta(x,y,t)\big|_{t=0} = \eta_0(x,y) \tag{14}$$

$$\nabla\phi(x,y,z,t)\big|_{t=0} = \nabla g(x,y,z) \tag{15}$$

where $\nabla g(x,y,z)$ denote the initial velocity potential and it should satisfy the irrotational condition. It is very difficult to solve Eq. (10) directly to study the wave kinematics and some simplification is necessary.

3.2 Simplified Treatment Method

Dommermuth and Yue (1987) presented an approximate model for wave motion. The velocity potential at wave surface is defined as (Zakharov. 1968):

$$\phi^s(x,y,t) = \phi(x,y,\eta(x,y,t),t) \tag{16}$$

where, $z=\eta(x,y,t)$ denotes the free surface. In terms of ϕ^s, the kinematic and dynamic boundary conditions on the free surface are respectively

$$\left.\begin{aligned} &\eta_t + \nabla_{\bar r}\phi^s \cdot \nabla_{\bar r}\eta - (1 + \nabla_{\bar r}\eta \cdot \nabla_{\bar r}\eta)\varphi_z(x,y,\eta,t) = 0 \\ &\phi^s_t + g\eta + \frac{1}{2}\nabla_{\bar r}\phi^s \cdot \nabla_{\bar r}\phi^s - \frac{1}{2}(1 + \nabla_{\bar r}\eta \cdot \nabla_{\bar r}\eta)\phi^2_z(x,y,\eta,t) = 0 \end{aligned}\right\} \tag{17}$$

where $\bar r=\{x,y\}$ is the position vector, $\nabla_{\bar r}=\left(\frac{\partial}{\partial x},\frac{\partial}{\partial y}\right)$ denotes the horizntal gradient.

The initial conditions at wave surface are

$$\phi(x,y,0) = q_1(x,y) \tag{18}$$

$$\eta(x,y,0) = q_2(x,y) \tag{19}$$

where $q_1(x,y)$ and $q_2(x,y)$ are given.

If the wave elevation, $\eta(x,y,t)$ and the velocity potential at free surface, $\phi^s(x,y,\eta,t)$ are expressed with the Fourier integral which satisfy the continuous equation and the bottom boundary condition, Eq. (17) is expressed as the equations concerning Fourier amplitude and these equations are solved by a perturbation method, whose key idea is that $\phi_z(x,y,\eta,t)$ is to be expressed as the function of ϕ and η. Dommermuth and Yue (1987) assumed that ϕ and η are $O(\varepsilon)$ quantities, where ε, a small parameter, is a measure of the wave steepness. We consider a consistent approximation up to and including a given order M in ε, and write ϕ in a perturbation series in ε.

The surface vertical velocity

$$\phi_z(x,y,\eta,t) = \sum_{m=1}^{M}\sum_{K=0}^{M-m}\frac{\eta^K}{K!}\sum_{n=1}^{N}\phi_n^{(m)}(t)\frac{\partial^{K+1}\psi_n(x,y,0)}{\partial z^K} \tag{20}$$

Substitute (20) into (17) and yields the final result

$$\left.\begin{aligned} &\eta_t + \nabla_{\bar r}\phi^s\nabla_{\bar r}\eta - (1 - \nabla_{\bar r}\eta \cdot \nabla_{\bar r}\eta)\left(\sum_{m=1}^{M}\sum_{K=0}^{M-m}\frac{\eta^K}{K!}\sum_{m=1}^{N}\phi_n^{(m)}(t)\frac{\partial^{K+1}\psi_n(x,y,0)}{\partial z^{K+1}}\right) = 0 \\ &\phi^s_t + \eta + \frac{1}{2}\nabla_{\bar r}\phi^s \cdot \nabla_{\bar r}\phi^s - \frac{1}{2}(1 + \nabla_{\bar r}\eta \cdot \nabla_{\bar r}\eta) \\ &\qquad\left(\sum_{m=1}^{M}\sum_{K=1}^{M-m}\frac{\eta^K}{K!}\sum_{n=1}^{N}\phi_n^{(m)}(t)\frac{\partial^{K+1}\psi_n(x,y,0)}{\partial z^{K+1}}\right)^2 = 0 \end{aligned}\right\} \tag{21}$$

Where $(\quad)^m$ denote a quantity of $O(\varepsilon^m)$, $\phi_n^{(m)}$ is called modal amplitude, $\psi_n(x,y,0)$ is given as follows:

$$\psi_n = \frac{\cosh k_n(z+d)e^{ik_n\vec{r}}}{\cosh k_n d} \tag{22}$$

where k_n is the wave number of nth characteristic wave. The modal amplitude, $\phi_n^{(m)}(t)$ can be treated as the function of ϕ^s and η and can be obtained by solving successively at increasing order the following equations

$$\left.\begin{aligned} &\sum_{n=1}^{N}\phi_n^{(1)}\psi_n(x,y,0) = \phi^s \\ &\sum_{n=1}^{N}\phi_n^{(m)}\psi_n(x,y,0) = \sum_{K=1}^{m-1}\frac{\eta^K}{K!}\left.\frac{\partial^K\left(\sum_{n=1}^{N}\phi_n^{(m-K)}\psi_n(x,y,z)\right)}{\partial z^K}\right|_{z=0} \\ &\qquad m = 2,3,\cdots,M \end{aligned}\right\} \tag{23}$$

Eq. (21) is the generalization to Mth order in wave steepness, ϵ of penturbation equations. For the finite ϵ, Dommermuth (1987) had proven that $|\psi_n(x,y,\eta_{max})/\psi_n(x,y,\eta_{min})|$ will rapidly increase along with n increasing. It means that the penturbation equation will exactly consistent coverge to the original equation.

For treating the three dimentional problem with both nonlinear and randomness the following model are proposed.

3.3 Wave Motion Equation under Known Wave Surface

When the surface elevations of a random wave are known, among two boundary condition equations at free surface only the potential function ϕ^s is to be determined. so we can choice either the kinematics boundary condition or the dynamic boundary condition as the boundary condition at known free surface. Thus the problem of solving velocity field under known wave surface is transformed into the boundary-value problem of Laplace equation in a given area, $x_1 \leqslant x \leqslant x_2$; $y_1 \leqslant y \leqslant y_2$; $-d \leqslant z \leqslant \eta(x,y)$ as Fig. 3 shown.

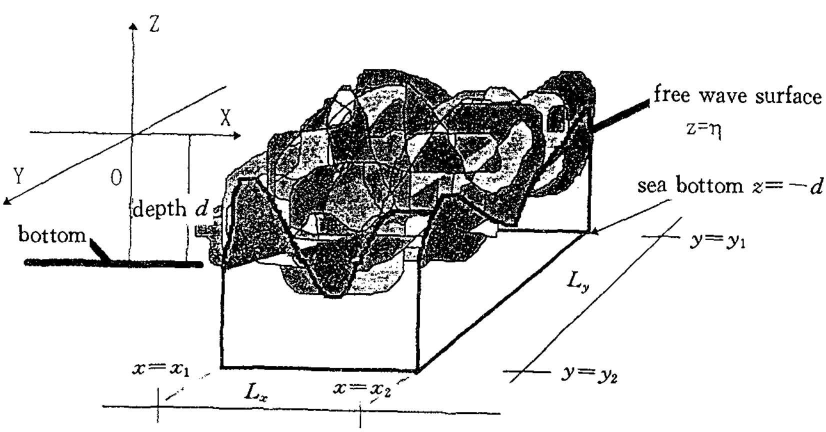

Fig. 3 Sketch of computation area

In given area, this boundary-value problem can be divided into two parts:

Part 1. Solve the surface protential function, $\phi^s(x,y,t)$ at free surface. Using Dommermuth's expression method, substituting (20) into (12), one can get the governing equation:

$$\eta_t = \sum_{m=1}^{M}\sum_{K=0}^{M-m}\frac{\eta^K}{K!}\sum_{n=1}^{N}\phi_n^{(m)}(t)\frac{\partial^{K+1}\psi_n(x,y,z)}{\partial z^{K+1}}\bigg|_{z=0} - \eta_x\phi_x^s - \eta_y\phi_y^s \tag{24}$$

Part 2. In the given area, solve the Laplace equaton given as Eq. (10). Their boundary conditions are

At bottom $z=-d$, as same as Eq. (11)

At free surface $z=\eta$, use the results in Part 1. The potential function at surface is used as the first kind of boundary condition.

At four profiles of $x=x_1, x=x_2, y=y_1$ and $y=y_2$ it is given directly by the linear potential function:

$$\phi(x,y,z,t) = \sum_{m=1}^{M}\sum_{i=1}^{I}\frac{a_{mi}g}{\omega_m}\frac{\cosh k_m(z+d)}{\cosh(k_m d)} \times \sin[k_m(x\cos\theta_i + y\sin\theta_i) + \omega_m t + \epsilon_{mi}] \tag{25}$$

As well know the accuracy of linear theory is enough except at where close free surface. If the computation area is large enough, the effect of the linear error on the computed results at the center point of this area can be negligible.

3.4 Numerical Method

The governing equation is solved with a finite diference method. Becaused the simplified governing equation is very simple, any special treatment is not needed for its computation.

3.4.1 Computing potential function at free surface.

At a given time the wave surface elevation, $\eta(x,y,t)$ and the linear potential function $\phi^s(x,y,t)$ are given so that the modal amplitude, $\phi_n^{(m)}(t)$ of velocity potential satisfys the Dirichirt boundary condition. Because the calculation reange is $z\leqslant 0$, so the amplitude $\phi_n^{(m)}(t)$ in the range of computational cuboid can be given with a pseudospectral method (Gottlieb and Orszag. 1977). The basic of the psendospectral method is the Fourier sesies expansion of periodic function and the Chebyshev polynomial expansion of a general function and the expansive coefficients are obtained with FFT. Here the FFT is done for wave number k (for frequency in general). In each order of solving proess, the number of k requested is equal to that of Fourier item.

For calculate $\phi_z^s(x,y,t)$, considering the nonlinear interaction between the component waves of different period, the order of the perturbation, M should be four. In this case, from Eq. (20) one can get:

$$\begin{aligned}\phi_z^s(x,y,t) = \sum_{n=1}^{N}e^{ik_n\bar{r}}\{&\phi_n^{(1)}[k_n\tanh(k_nd) + \eta k_n^2 + \frac{\eta^2}{2}k_n^3\tanh(k_nd) + \frac{\eta^3}{6}k_n^4]\\ &+ \phi_n^{(2)}[k_n\tanh(k_nd) + \eta k_n^2 + \frac{\eta^2}{2}k_n^3\tanh(k_nd)]\\ &+ \phi_n^{(3)}[k_n\tanh(k_nd) + \eta k_n^2] + \phi_n^{(4)}[k_n\tanh(k_nd)]\}\end{aligned} \tag{26}$$

Then calculate ϕ' at discrete points with iterative method.

3.4.2 Calculate ϕ in the given area.

3.4.3 Matching the boundary conditions

At the boundary between free surface and four profiles of $x=x_1$, $x=x_2$, $y=y_1$ and $y=y_2$ the boundary conditions are not continuative. Because the potential function at free surface is obtained by Eq. (24) and those at four profiles are given by linear wave theory. The Lagrange's insertion formula is used to matching the boundary conditions. For the deep water take the bottom bonndary at $z=-\frac{d}{2}$ and the potential function is also given by linear theory, it is in harmony with that at four profiles.

3.4.4 Solve difference equation group

The successive overrelaxation (SOR) method is used to solve the difference equation. The relaxation factor is equal to 1.5.

3.5 Reliability Examination of Numerical Method.

3.5.1 Errors due to linear boundary conditions

A regular wave is considered, its $H=15$cm, $T=1.5$s and depth $d=41.3$m. Two boundary conditions are artificially constructed, one is a linear boundary and at the boundary between wave surface and four profiles, the boundary conditions are matching with Lagrange's insertion. Another is taken as $\phi_0(z) \cdot G(z)$ and the definition of $G(z)$ is shown in Fig. 4(a). The computational parameters are perturbation order $M=3$, Fourier trunction number $N=16$. Computation area $x_1=0$, $x_2=2.0$m, node spacing $\Delta x=0.05$m, $\Delta z=0.01$m. Fig. 4(b) shows that the potential functions $\phi(i,j)$ at different depth obtained from linear boundary condition are in agreement with that obtained from another boundary condition beyond the eighth node. So it is concluded that for calculating the potential function at the center of area 2×2m the linear boundary condition is available with enough accuracy.

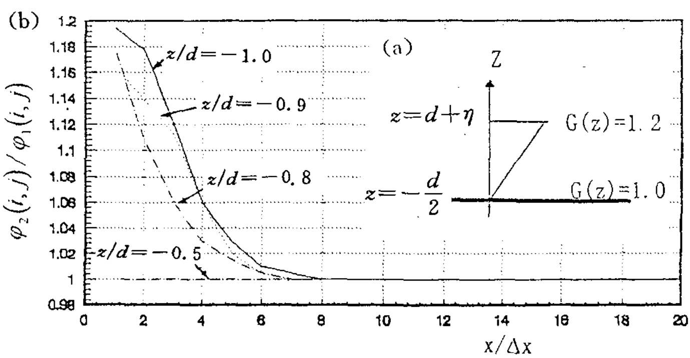

Fig. 4 Errors due to linear boundary condition

3.5.2 The effect of perturbation order number M

Taking $M=1,2,3$ and 4 respectively calculate the velocity v_x in a regular wave as above mentioned at $x=1.0$m, $z/d=-0.25$. As Fig. 5 shows that the velocity for $M=3$ is almost the same as that for $M=4$ and even if $M=2$ its result is acceptable.

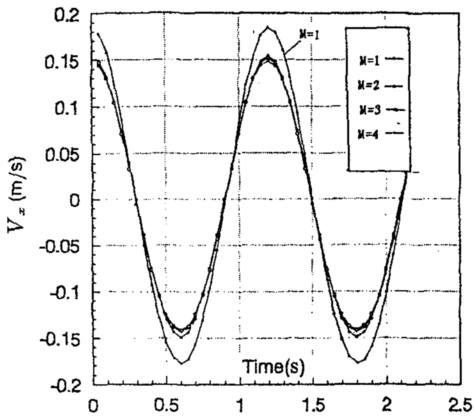

Fig. 5 Comparison of calculation results with different M for velocity V_x

3.5.3 Comparison between numerical calculation and wave theories

The linear theory, 2nd Stokes and 3rd Stokes wave theories and the numerical method are used to calculate the velocity v_x respeitively in a regular wave. The results show that at the crest phase the velocity v_x calculated by numerical method is almost the same as that from 3rd Stokes wave theory.

3.6 Velocity Field in 3-D Random Waves—Model Test

The velocity field in regular wave, unidirectional random wave and 3-D random wave were experimentally studied in the State Key Laboratory of Coastal and Offshore Engineering, Dalian University of Technology, China. The wave basin is 55m long, 34m wide and 1.3m deep. The multi-directional wave-maker consists of 70 independent segments of 0.4m wide. Wave absorbers were placed along the basin walls to prevent wave reflection from the walls. A wave gage array consisted of 8×8 gages was set 6.5m apart from the wave plate. The gage spacings were about 0.25m. An Acoustic Doppler Velocimeter (ADV) was put near the center of the wave gage array to measure three flow velocity components. The data of wave elevations and velocities were acquired simultaneonsly by computer. The sampling interval was 0.05s and the data length is 512—1024 (regular waves)、4096(unidirectional waves) and 8192 points (3-D random waves). The water depth was kept 0.413m. The velocities were measured at $Z=-0.303$m, -0.196m, -0.109m and -0.018m respectively. For the last case, the ADV was out of water at trough phase.

The JONSWAP spectrum, $\gamma=3.3$ and the Mitsuyasu-type spreading function, $G_0\cos^{2s}\frac{\theta}{2}$, was used to simulate the 3-D random waves with the Single Direction Per Frequency Model (Yu et al, 1991). $H_{\frac{1}{3}}=0.047\sim0.145$m, $T_{H\frac{1}{3}}=1.09\sim$

1.88s. The measured directional spectrum was estimated by the Bayesian Approah (Hashimoto et al, 1987). The numerical inversion method was used to obtain the wave surface at ADV's position from the wave surfaces at 5 near locations. Then it was used to claculated the velocities and comparied with the measured ones by ADV.

Fig. 6 shows an example of the comparisom between calculated and measured velocity hostories in an oblique 2-D random wave. Two velocity histories are agreeable each other.

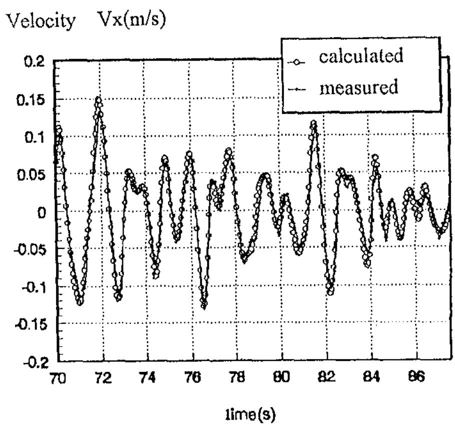

Fig. 6 Comparison between calculated and measured velocity histories in an oblique random wave

The example of the compareson between the calculated and measured velocities v_x, v_z in a 2-D random wave at the position $z=-0.018$m is shown in Fig. 7. Two sets of velocity history are agreeable. But for the trough phase, the ADV is out of the water so the measured velocities are equal to zero.

For the 3-D random waves the example of the comparison between the measured and calculated velocities is shown in Fig. 8. The wave spreading parameter, $s=50$. The velocities are measured at the position 0.304m above bottom. Two sets of velocity history are basically consistent. In this case the accuracy of velocity calculation is also dependent on that of the wave surface inversion.

3.7 Effects of nonlinearity on velocity

For the unidirectional wave, the direct linear method and Donelan's linear method (1992) are used to calculate the velocities at different depth and their results are compared with that by the nonlinear numerical method. Their ratios are shown in Fig. 9. The measured results are also shown in this figure by closed circles. It is found that when $z/d<-0.25$ all of three methods can predict the avaible velocities which is close to the measured ones. But when $z/d\rightarrow 0$ two linear

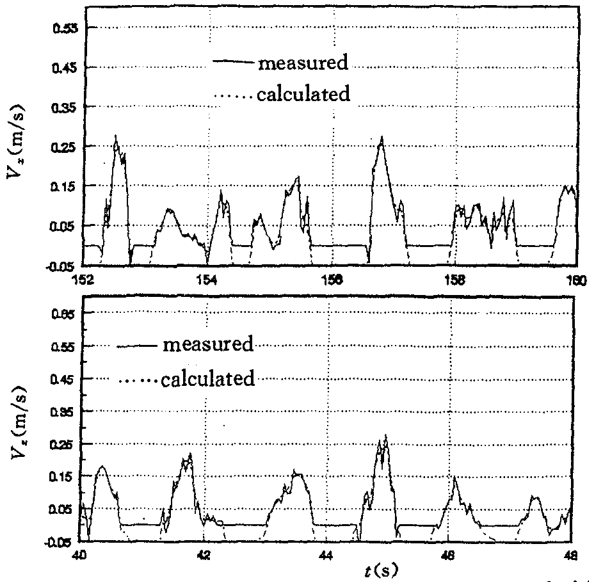

Fig. 7 Comparison between calculated and measured velocities in a 2-D random wave (H_s=4. 88cm, T_s=1. 39s)

mthods over-predict the velocities. For 3-D waves, the general variation tendency is the same as for 2-D waves.

Fig. 10 shows the comparison between calculated and measured velocities v_x and v_y at wave crest for 3-D random wave. The linear method overestimate the velocities and the nonlinear numerical method predict the velocities closed to measured ones.

4. CONCLUSIONS

A numerical method calculating the 3-D velocity field under a given random wave surface directly by the governing equations is proposed in this paper. It is verified with the exprimental study that this methed can predicte 3-D velocities at different locations including wave crest with high accuracy. The direct linear method usually greatly overestimates the crest velocities near the surface.

The wave surface needed for velocity calculation can be numerically simulated from directional spectrum or determined from other wave surfaces at near locations with an inversion method proposed in this paper. The inversion method is verified with model test and field data.

The effects of nonlinearity of waves on the velocities at positions near still water level are not negligible. The experimental results show that this effect of 2-D waves is more than that of 3-D waves and this effect on vertical component velocity is more than that on horizontal component velocity.

Acknowledgments—This project is supported by the Foundation of State Key

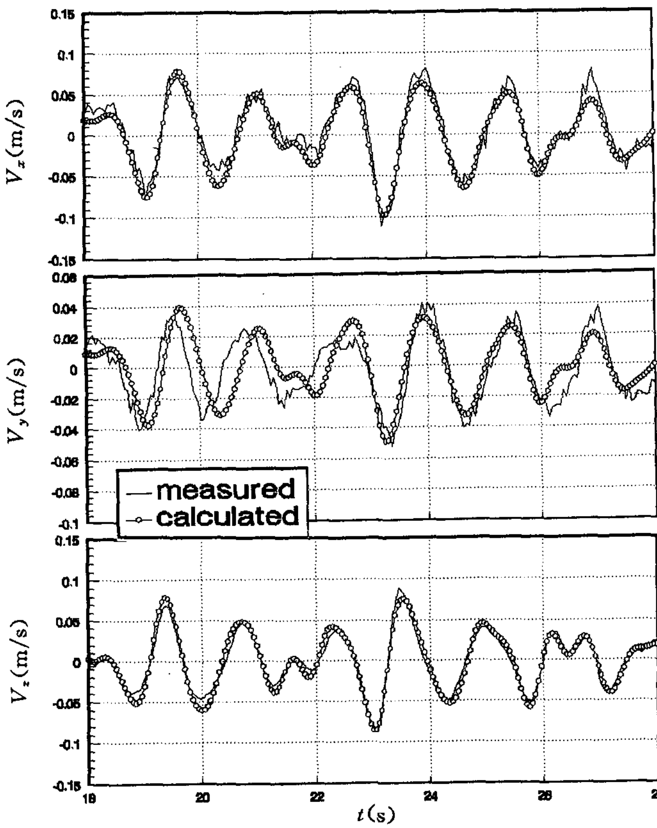

Fig. 8 Comparison between calculated and measured velocity histories in 3-D wave (H_s=5.1cm, T_s=1.38s, s=50, d=41.3cm, z=−10.9cm)

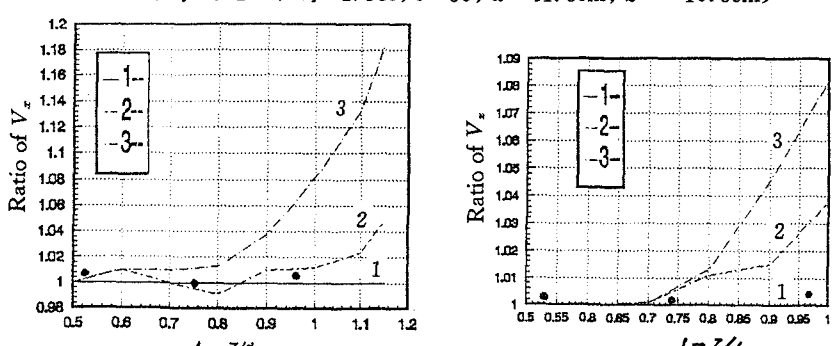

Fig. 9 Effects of nonlinearity on velocities V_x and V_z (H/d=0.36, H/L=0.122, 1-nonlinear method; 2-Donelan; 3-direct linear method)

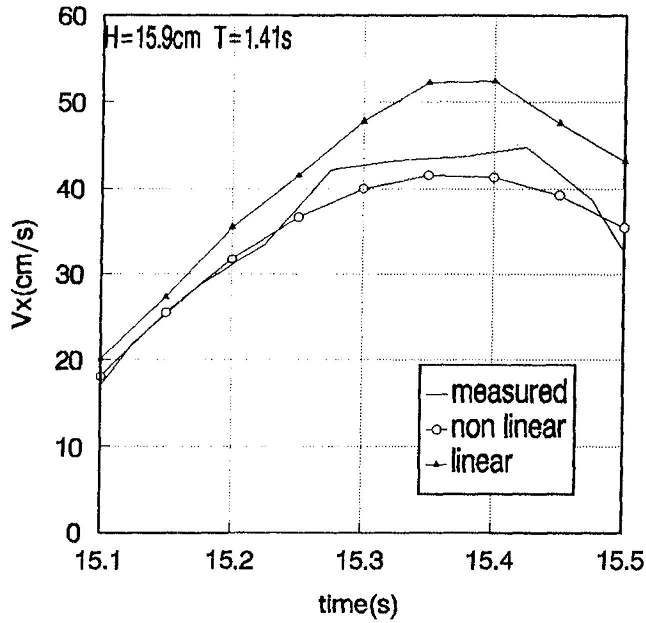

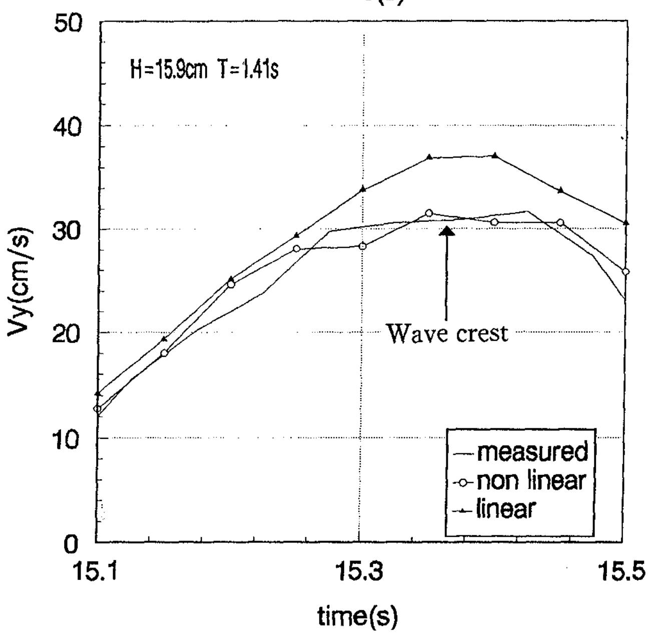

Fig. 10 Comparison between calcualted and measured velocities v_x and v_y at wave crest for 3-D wave.
(d=41.3cm, z=−1.8cm, H_s=12.3cm, T_s=1.39s)

Laboratory of Coastal and Offshore Engineering, China. The anthors sincecely wish to express their appreciation to Mrs. Y. Sun, M. N. Go and Mr. Z. C. Jiang for their great helps to this study.

REFERENCES

Dommermuth D. G. and Yue K. P. ,(1987), A high-order spectral method for the study of nonlinear gravity waves. J. Fluid Mech. Vol. 184, 267-288.

Donelan M. A. , Anctil F. and Doering J. C. (1992). A simply method for calculating the velocity field beneath irregular waves, Coastal Engineering, 16, 199-224.

Forristall G. Z. , Ward E. G. , Cardone, V. J. Borgmann, L. E. (1978), The directional spectra and kinematics of surface gravity waves in tropical storm Delia, J. Phys. Ocean, 8. 888-909.

Gottlieb, D. and Orszag, S. A. (1977), Numerical analysis of spectral methods, SIAM.

Hashimoto N. , Kobune, K. , Kambyama Y. (1987), Estimation of directional spectrum using the Bayesian Approach and its application to field data analysis, Report of the Port and Harbour Research Institute. Vol. 12, 57-100.

Prislin I. and Zhang J. (1997), Pridiction of wave kinematics under the wave crest in short-crested irregular gravity waves, IAHR Seminar, Multidirectional Waves and Their Interaction with Structures, 357-370.

Rodenbuch G. and Forristall, G. E. , (1982). Three crest kinematics models compared to MaTS data and OTS data. MaTS Report VM-1-4B. Netherlands Marine Technological Research Program.

Yu, Y.X. , Lin S.X. and Li L. (1991), Numerical simulation of multidirectional random waves. Proc. 1st Inter. Offshore and Polar Engineering Conf. 26-32.

Zakharov V. E. (1968),Stability of periodic waves of finite amplitude on the surface of a deep fluid. J. Appl. Mech. Tech. Phys. 9, 190-194.